IV Journeys in Multiphase Flows (JEM 2017)
March 27-31, 2017, São Paulo, SP, Brazil

Paper ID: JEM-2017-0016

EVALUATION OF THE GAS CONTRIBUTION TO THE MOMENTUM AND ENERGY BALANCES FOR LIQUID-GAS SLUG FLOWS IN HIGH PRESSURE SCENARIOS USING A MECHANISTIC APPROACH

Carlos L. Bassani, langebassani@gmail.com
Fernando H.G. Pereira, fernandopereira@alunos.utfpr.edu.br
Fausto A.A. Barbuto, fausto_barbuto@yahoo.ca
Rigoberto E.M. Morales, rmorales@utfpr.edu.br
Multiphase Flow Research Center (NUEM), Federal University of Technology – Paraná (UTFPR), Rua Deputado Heitor Alencar Furtado 5000, Bloco N, CEP 81280-340, Curitiba/PR, Brazil.

Abstract. *The heat transfer between the deep sea waters and the oil and gas mixtures flowing through production lines is a day-to-day situation in the petroleum industry. The optimum prediction of the liquid-gas flow parameters along those lines, where the slug flow pattern is predominant, has an extreme importance in the design of production facilities. The mixture temperature drop caused by the colder sea waters directly affects physical properties of the fluids such as the viscosity and specific mass. Gas expansion may also occur due to pressure and temperature gradients, thus changing the flow hydrodynamics. Several models have been developed to characterize this kind of flow along the pipeline. When dealing with long pipelines, it is important to choose a less expensive model, such as the mechanistic ones. These models are, however, not yet prepared for taking the gas contribution in momentum and energy balances into account – which cannot be neglected when dealing with the frequently high pressures found at the inlet of long pipelines. With this challenge in mind, the present work extends a mechanistic approach for characterizing the slug flow hydrodynamics and heat transfer to account for the effects brought by the gas to the conservation equations, with a special focus on the energy balance. Terms due to the gas expansivity, the gas heat capacity and the heat transfer between the gas and the wall are introduced in the model. Results are shown as to evidence the gas contribution in higher pressure scenarios, when the gas contribution is not negligible. The parameters analyzed are the mixture temperature, pressure and heat transfer coefficient and the gas superficial velocity.*

Keywords: *gas-liquid slug flow, heat transfer, high pressure, long distance pipeline, mechanistic approach.*

1. NOMENCLATURE

Roman letters

A	Cross sectional area	[m^2]
c	Specific heat	[J/(kg.K)]
D	Diameter	[m]
$freq$	Slug flow frequency	[Hz]
h	Heat transfer coefficient	[W/(m^2.K)]
j	Phase superficial velocity	[m/s]
J	Mixture superficial velocity	[m/s]
k	Thermal conductivity	[W/(m.K)]
K	Head loss coefficient	[-]
L	Length	[m]
$\dot{m}$	Mass flow rate	[kg/s]
P	Pressure	[Pa]
R	Phase volumetric fraction	[-]
S	Wetted perimeter	[m]
T	Temperature	[K]
U	Real velocity	[m/s]
z	Pipe axial coordinate	[m]
Z	Compressibility factor	[-]

Greek letters

γ	Pipe inclination	[rad]
κ	Thermal scooping factor	[-]
μ	Viscosity	[Pa.s]
ρ	Density	[kg/m^3]
τ	Shear stress	[Pa]
ϕ	Phase ($\phi = L;G$)	
ψ	Slug region ($\psi = B;S$)	

Indexes

B	Bubble region
ext	External medium
f	Front
i	Gas-water interface
G	Gas
L	Liquid
m	Mixture
n	Node index
$ov.$	Overall
r	Rear
S	Slug region
T	Unit cell translation
U	Unit cell
W	Wall

2. INTRODUCTION

Slug flow is a gas-liquid two-phase flow pattern that occurs over a wide range of gas and liquid flow rates. It is characterized by the intermittent succession of two bodies: a liquid slug, which may or may not contain dispersed gas bubbles in it, and an elongated bubble sliding over a thin liquid film. Together, those two structures constitute that what is known as a *unit cell* (Shoham, 2006). The slug and the elongated bubble possess characteristic velocities and geometric features such as lengths and phase fractions. Those characteristics depend on time and space and their prediction is central in the design of facilities for industrial applications such as nuclear power plants and oil and gas transportation systems.

Several approaches have been used to model slug flows, namely: steady-state mechanistic models (Bassani et al., 2016; Cook and Behnia, 2000; Medina et al., 2010; Shoham, 2006; Taitel and Barnea, 1990), Eulerian transient drift flux models (Danielson, 2011; Zerpa et al., 2013), Eulerian transient two-fluid models (Issa and Kempf, 2003; Simões et al., 2014), Lagrangian transient slug tracking models (Medina et al., 2015; Nydal and Banerjee, 1996; Taitel and Barnea, 1998) and hybrid models (Kjeldby et al., 2013). However, only a few of those studies consider heat transfer (Bassani et al., 2016; Medina et al., 2015; Simões et al., 2014; Zerpa et al., 2013), and their development is still recent in literature. Low-cost and stable computational models such as the mechanistic ones become even more important when long distance pipelines are brought into play. However, the aforementioned kind of model is not yet prepared to take into account some important phenomena that happen in long-distance pipelines scenarios.

The mechanistic model that will be used as the guide for the present study (Bassani et al., 2016) neglects the gas phase contribution to the energy balance by assuming that the gas density is negligible when compared to the liquid one. This is a fair assumption when dealing with low pressure scenarios, near ambient conditions. However, this is not the case of long-distance pipelines, where high pressures are present especially at the pipe inlet section. In this case, the gas contribution cannot be neglected and needs to be modeled.

The present work is an improvement over the steady-state mechanistic model proposed by Bassani et al. (2016) for accounting the gas contribution to the conservation equations. In the mass conservation, the compressibility factor of the gas is taken into account to recalculate the gas superficial velocity along the pipeline due to pressure and temperature variations. In the energy balance, the gas is assumed as real, with an extra term to account for its expansivity. The gas contribution to the other terms of the energy balance – namely the gas heat capacity, the thermal scooping phenomenon and the heat transfer with the wall – will also be included in the present study. This work attempts to join the low computational cost and numerical stability of the steady-state mechanistic models with the phenomena related to the gas contribution to the conservation equations – which are already taken into account in transient models with higher computational costs.

3. MATHEMATICAL MODEL

Figure 1a depicts a typical horizontal slug flow. This flow pattern is characterized by the intermittent succession of *unit cells* constituted of two regions, herein designated by ψ: the *elongated bubble* (*B*) and the *slug* (*S*). Each region may contain both phases, that is, the *gas* (*G*) and the *liquid* (*L*), designated by ϕ. Each phase inside each region is called a *unit cell structure* $\phi\psi$, being: the *gas in the elongated bubble* (*GB*), the *liquid film that flows underneath the elongated bubble* (*LB*), the *liquid in the slug body* (*LS*) and the *gas bubbles dispersed in the slug body* (*GS*).

Figure 1b presents the characterization of the problem. The pipeline is divided in nodes spaced by Δz. The superficial velocities of the phases and the mixture pressure and temperature are assumed to be known at the pipe inlet. The pipeline is cooled externally by an infinite medium of nearly constant temperature and heat transfer coefficient – the ocean. The pipeline is assumed to be horizontal.

Knowing the superficial velocities of the phases, the unit cell geometry can be estimated by the Taitel and Barnea's (1990) approach. The unit cell geometry is related to: (i) the volumetric fraction of the phases in each region and (ii) the region lengths. The knowledge of the phases' distribution is paramount for predicting their real velocities inside each region of the unit cell by means of a mass balance. By their turn, the real velocities are used to find: (i) the shear stresses of the structures for estimating pressure in the next node, using a momentum balance; and (ii) the heat transfer coefficient of the structures for estimating the mixture temperature in the next node, using an energy balance. The gas superficial velocity can then be recalculated for the next node, accounting for the gas expansion or contraction due to both pressure and temperature gradients. The liquid is assumed as incompressible, thus its superficial velocity is constant. Once temperature, pressure and superficial velocities of the phases in the next node are known, the process can be repeated until the last node of the pipeline is reached, following an upwind-wise logic.

3.1 Hydrodynamic model

The momentum balance for the phase ϕ in the elongated bubble region is stated as (Taitel and Barnea, 1990):

$$\rho\left|U_T-U_{\phi B}\right|\frac{\partial\left(U_T-U_{\phi B}\right)}{\partial z}=-\frac{\partial P}{\partial z}A\cos\theta dz+\frac{\tau_{\phi B}S_{\phi B}}{A}\pm\frac{\tau_i S_i}{A}+\rho g\sin\theta-\rho g\cos\theta\frac{\partial H_{\phi B}}{\partial z} \tag{1}$$

being $\tau_{\phi\psi}$ the shear stresses of each structure, $A_{\phi\psi}$ the cross sectional areas occupied by those structures, $S_{\phi\psi}$ their wetted perimeters, $R_{\phi\psi}$ their volumetric fractions and γ the pipe inclination. Applying for both phases $\phi=L,G$, knowing that $H_{LB}+H_{GB}=D$ – that is, the film height plus the bubble height equals the pipe internal diameter – and considering a constant pressure in the cross sectional area, one can find an ODE for the liquid film height H_{LB} as a function of the pipe axial coordinate z (Taitel and Barnea, 1990):

$$\frac{dH_{LB}}{dz}=\frac{\dfrac{\tau_{LB}S_{LB}}{A_{LB}}-\dfrac{\tau_{GB}S_{GB}}{A_{GB}}-\tau_i S_i\left(\dfrac{1}{A_{LB}}+\dfrac{1}{A_{GB}}\right)+\left(\rho_L-\rho_G\right)g\sin\gamma}{\left(\rho_L-\rho_G\right)g\cos\gamma-\rho_L\dfrac{\left|U_T-U_{LB}\right|\left(U_T-U_{LB}\right)}{R_{LB}}\dfrac{dR_{LB}}{dH_{LB}}-\rho_G\dfrac{\left|U_T-U_{GB}\right|\left(U_T-U_{GB}\right)}{R_{GB}}\dfrac{dR_{LB}}{dH_{LB}}} \tag{2}$$

This ODE can be numerically integrated until convergence with the liquid mass balance inside the unit cell. The liquid mass balance of the entire unit cell – estimated via the liquid superficial velocity – shall be equal to the sum of the film and the slug region mass balances (Taitel and Barnea, 1990):

$$\underbrace{\dot{m}_{LU}=\rho_L A j_L}_{\text{unit cell}}=\underbrace{\rho_L A R_{LS}U_{LS}\frac{L_S}{L_U}}_{\text{slug}}+\underbrace{\rho_L A\frac{1}{L_U}\int_0^{L_B}R_{LB}U_{LB}dz}_{\text{film}} \tag{3}$$

Equations (2) and (3) are used to characterize the unit cell geometry, that is, the region lengths and its phase fractions. The model closure is reached by means of some experimental correlations that estimate the slug flow frequency (Schulkes, 2011), the unit cell translational velocity (Petalas and Aziz, 1998) and the gas fraction in the slug body (Andreussi et al., 1993).

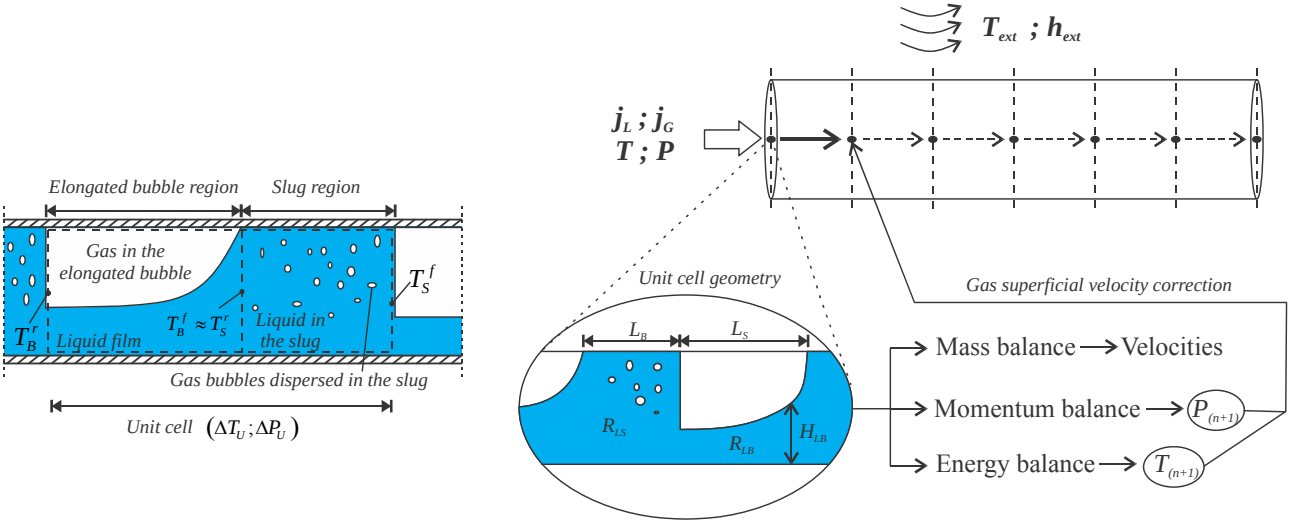

Figure 1 – (a) Unit cell with its respective regions and flow structures. (b) Problem characterization for slug flow hydrodynamics and heat transfer calculations.

The real velocities of the liquid film U_{LB} and of the gas in the elongated bubble U_{GB} are found by the mass conservation, eq. (4) (Taitel and Barnea, 1990). Assuming that the liquid slug body carries the gas dispersed bubbles and that no slippage occurs, the velocities of these structures can be considered equal – assumption valid for horizontal flow (Harmathy, 1960). As a consequence of this assumption, the slug body and the mixture J travel at the same velocity (Shoham, 2006), being the latter defined as the sum of the liquid and the gas superficial velocities, eq. (5). Whereas the liquid superficial velocity can be assumed as nearly constant due to the incompressible behavior of this

phase, the gas superficial velocity needs to be corrected throughout the pipeline due to pressure and temperature variations, eq. (6).

$$U_{LB} = U_T - \left(U_T - U_{LS}\right)\frac{R_{LS}}{R_{LB}} \;;\; U_{GB} = U_T - \left(U_T - U_{GS}\right)\frac{\left(1-R_{LS}\right)}{R_{GB}} \tag{4}$$

$$U_{GS} \approx U_{LS} \approx J = j_G + j_L \tag{5}$$

$$j_{L(n+1)} = j_{L(n)} \;;\; j_{G(n+1)} = j_{G(n)}\frac{Z_{(n+1)}}{Z_{(n)}}\frac{P_{(n)}}{P_{(n+1)}}\frac{T_{(n+1)}}{T_{(n)}} \tag{6}$$

where (n) and ($n+1$) are node indexes and Z is the gas compressibility factor. Equation (6) was modified from the original work (Bassani et al., 2016) to accommodate the gas real behavior.

Finally, the pressure variation between two consecutive nodes can be estimated by the momentum balance in the unit cell, related to: (i) the friction between each structure and the wall (Taitel and Barnea, 1990), (ii) the friction between the phases and (iii) the pressure drop related to the recirculation in the wake zone behind the elongated bubble (Cook and Behnia, 2000):

$$P_{(n+1)} = P_{(n)} - \left[\underbrace{\frac{\tau_{LS}S_{LS}}{A}\frac{L_S}{L_U}}_{\substack{\text{friction in the}\\ \text{slug region}}} + \underbrace{\frac{\left(\tau_{LB}S_{LB} + \tau_{GB}S_{GB} + \tau_i S_i\right)}{A}\frac{L_B}{L_U}}_{\text{friction in the elongated buble region}} + \underbrace{K\rho_L\frac{\left(U_{LB}-U_T\right)^2}{2L_U}}_{\substack{\text{head loss in the}\\ \text{elongated bubble rear}}}\right]\Delta z \tag{7}$$

The difference between eq. (7) and the original work (Bassani et al., 2016) is the inclusion of the gaseous and the gas/liquid interface friction. Those terms had already been considered in the pioneer work of Taitel and Barnea (1990). However, Taitel and Barnea (1990) did not consider the head loss term in the wake zone of the elongated bubble. Equation (7) unifies all those terms in an expression for the pressure distribution along the pipeline.

3.2 Heat transfer model

Neglecting heat generation, the energy conservation equation in its differential form can be expressed as:

$$\underbrace{\rho c_P\frac{DT}{Dt}}_{\text{(I)}} = \underbrace{\nabla\cdot\left(k\nabla T\right)}_{\text{(II)}} + \underbrace{\beta T\frac{DP}{Dt}}_{\text{(III)}} + \underbrace{\mu\Phi}_{\text{(IV)}} \tag{8}$$

where c_P is the specific heat, k is the thermal conductivity, T is the temperature and β is the coefficient of thermal expansion. Each term of eq. (8) will be modeled in a separated subsection.

Energy variation

Term (I) of eq. (8) represents the energy variation inside the unit cell, which can be expanded as the energy variation along time plus the energy crossing the unit cell borders – also known as *thermal scooping phenomenon* (Bassani et al., 2016):

$$\rho c_P\frac{DT}{Dt} = \underbrace{\rho c_P\frac{dT}{dt}}_{(i)} + \underbrace{\rho c_P u\frac{dT}{dz}}_{(ii)} \tag{9}$$

being u the relative velocity between the phase and the control volume. Since the control volume of Fig. 1a displaces with the unit cell translational velocity U_T, then the temperature variation with time can be written as $dT/dt = U_T\,dT/dz$ (Bassani et al., 2016). Using a homogeneous approach, term (i) can be rewritten as:

$$\rho c_P\frac{dT}{dt} \approx \rho_m c_{P,m} U_T\frac{dT}{dz} \tag{10}$$

where the index m refers to the mixture. Term (ii) of eq. (9) represents the net transfer of energy through the borders of the control volume and can be rewritten as:

$$\rho c_P u \frac{dT}{dz} \approx -\rho_m c_{P,m}\left(J-U_T\right)\left(T-\frac{\Delta T_U}{2L_U}\right)+\rho_m c_{P,m}\left(J-U_T\right)\left(T+\frac{\Delta T_U}{2L_U}\right)=\rho_m c_{P,m}\left(J-U_T\right)\frac{\Delta T_U}{L_U} \tag{11}$$

being $(J-U_T)$ the relative velocity between the mixture and the control volume that encloses the unit cell. Separating the contributions of both phases $\phi = L, G$:

$$\rho c_P u \frac{dT}{dz} \approx \sum_\phi \rho_\phi c_{P,\phi} R_{\phi\psi}\left(U_{\phi\psi}-U_T\right)\frac{\Delta T_U}{L_U} \tag{12}$$

Using the hypothesis that the mass fluxes entering and exiting the unit cell borders can be considered equal (Taitel and Barnea, 1990), eq. (12) can be rewritten as function of either the elongated bubble or the slug region:

$$\rho c_P u \frac{dT}{dz} \approx \sum_\phi \rho_\phi c_{P,\phi} R_{\phi B}\left(U_{\phi B}-U_T\right)\frac{\Delta T_U}{L_U} \approx \sum_\phi \rho_\phi c_{P,\phi} R_{\phi S}\left(U_{\phi S}-U_T\right)\frac{\Delta T_U}{L_U} \approx \sum_\phi \frac{\dot{m}_{\phi z} c_{P,\phi}}{A}\frac{\Delta T_U}{L_U} \tag{13}$$

being $\dot{m}_{\phi z} \approx \rho_\phi A R_{\phi B} \approx \rho_\phi A R_{\phi S}(U_{\phi B}-U_T)$ the mass flow rate between two consecutive unit cells, also known as *scooping mass flow rate* (Taitel and Barnea, 1990). Expanding the sum of eq. (13) for both phases $\phi = L, G$ and adopting the elongated bubble region as reference:

$$\rho c_P u \frac{dT}{dz} \approx \left(\dot{m}_{Lz} c_{P,L} + \dot{m}_{Gz} c_{P,G}\right)\frac{\Delta T_U}{AL_U} \tag{14}$$

The temperature difference between the two unit cell borders ΔT_U can be estimated through the wall-mixture temperature difference $(T_W - T)$ and the *thermal scooping factor* κ as $\Delta T_U = \kappa\left(T_W - T\right)$ (Bassani et al., 2016). The scooping factor can be modeled by applying an energy balance in the slug and in the elongated bubble regions. Considering that the structures translate at a velocity near the mixture superficial velocity *J*, a relation between the temperatures at the borders of each region can be found when integrating the energy balance along the region lengths:

$$\frac{T_W - T_S^f}{T_W - T_S^r} = \exp\left(-\frac{h_{LS} S_{LS} L_S}{\rho_{mS} c_{P,m} AJ}\right) \; ; \; \frac{T_W - T_B^f}{T_W - T_B^r} = \exp\left(-\frac{h_{LB} S_{LB} L_B + h_{GB} S_{GB} L_B}{\rho_{mB} c_{P,m} AJ}\right) \tag{15}$$

where the indexes *f* and *r* refer to the front and rear of the regions, respectively. The mixture density in the slug and in the elongated bubble regions is calculated by means of a mass balance as $\rho_{mS} = \rho_L R_{LS} + \rho_G R_{GS}$ and $\rho_{mB} = \rho_L R_{LB} + \rho_G R_{GB}$, respectively. The mixture specific heat is estimated by an energy balance as $c_{P,m} = \left(\rho_L j_L c_{p,L} + \rho_G j_G c_{p,G}\right) / \left(\rho_L j_L + \rho_G j_G\right)$. Reorganizing the terms so as to find an expression for $\Delta T_U = T_{LS}^f - T_{LB}^r$ and then dividing by $\left(T_W - T\right)$, the thermal scooping factor becomes:

$$\kappa = \exp\left(\frac{h_{LB} S_{LB} L_B + h_{GB} S_{GB} L_B}{\rho_{mB} c_{P,m} AJ}\right) - \exp\left(-\frac{h_{LS} S_{LS} L_S}{\rho_{mS} c_{P,m} AJ}\right) \tag{16}$$

The main difference between eq. (16) and the original work (Bassani et al., 2016) is the contribution of the gaseous phase, i.e., term expressed by $h_{GB} S_{GB} L_B$. Finally, substituting eqs. (10) and (14) in (9), an expression for the energy variation inside the unit cell is found:

$$\rho c_P \frac{DT}{Dt} \approx \rho_m c_{P,m} U_T \frac{dT}{dz} + \left(\dot{m}_{Lz} + \dot{m}_{Gz}\right)\frac{\kappa\left(T_W - T\right)}{AL_U} \tag{17}$$

Heat transfer with the wall

Term (II) of eq. (8) is related to the heat transfer between the mixture and the wall. Weighing the contribution of each flow structure by the region lengths and considering the same mixture-wall temperature gradient:

$$\nabla\cdot\left(k\nabla T\right)\approx\frac{1}{A}h_m S\left(T_W-T\right)\approx\frac{1}{A}\sum_{\phi,\psi}h_{\phi\psi}S_{\phi\psi}\frac{L_\psi}{L_U}\left(T_W-T\right)=\frac{1}{AL_U}\left(h_{GB}S_{GB}L_B+h_{LB}S_{LB}L_B+h_{LS}S_{LS}L_S\right)\left(T_W-T\right) \tag{18}$$

Expansivity of the phases

Term (III) of eq. (8) represents the contribution of the expansivity of the phases on the energy balance and can be written as:

$$\beta T\frac{DP}{Dt}=\underbrace{\beta T\frac{dP}{dt}}_{(iii)}+\underbrace{\beta Tu\frac{dP}{dz}}_{(iv)} \tag{19}$$

The steps followed for modeling terms (iii) and (iv) are analogous to the steps used by term (i) and (ii) of eq. (9), respectively. Term (iii) represents the expansivity of the mass content inside the control volume. Using $dP/dt=U_T\,dP/dz$, separating the contributions of each phase and knowing that the volumetric flow rate of the phases inside the unit cell is $\dot{m}_{\phi U}=\rho_\phi AR_{\phi U}U_T$, then:

$$\beta T\frac{dP}{dt}\approx\beta TU_T\frac{dP}{dz}=\sum_\phi\beta_\phi R_{\phi U}TU_T\frac{dP}{dz}=\left(\beta_L R_{LU}+\beta_G R_{GU}\right)TU_T\frac{dP}{dz}=\left(\frac{\beta_L}{\rho_L}\dot{m}_{LU}+\frac{\beta_G}{\rho_G}\dot{m}_{GU}\right)\frac{T}{A}\frac{dP}{dz} \tag{20}$$

Term (iv) of eq. (19) represents the expansivity contribution in the energy balance due to the pressure variation between the borders of the control volume. That is, even if the mass flow rate $\dot{m}_{\phi z}$ entering and exiting the unit cell is considered equal, the pressure at each border is different. The pressure gradient along the unit cell can be considered as nearly constant, then $\Delta P_U=L_U\,dP/dz$, thus yielding:

$$\beta Tu\frac{dP}{dz}\approx-\beta_m T\left(J-U_T\right)\left(P-\frac{\Delta P_U}{2L_U}\right)+\beta_m T\left(J-U_T\right)\left(P+\frac{\Delta P_U}{2L_U}\right)=\beta_m T\left(J-U_T\right)\frac{dP}{dz} \tag{21}$$

Separating the contribution of each phase, rewriting in terms of the scooping mass flow rates and adopting the elongated bubble region as reference:

$$\beta Tu\frac{dP}{dz}\approx\sum_\phi\beta_\phi R_{\phi B}\left(U_{\phi B}-U_T\right)T\frac{dP}{dz}=\left[\beta_L R_{LB}\left(U_{LB}-U_T\right)+\beta_G R_{GB}\left(U_{GB}-U_T\right)\right]T\frac{dP}{dz}=\left(\frac{\beta_L}{\rho_L}\dot{m}_{Lz}+\frac{\beta_G}{\rho_G}\dot{m}_{Gz}\right)\frac{T}{A}\frac{dP}{dz} \tag{22}$$

Finally, substituting eqs. (20) and (22) in (19) and neglecting the liquid compressibility, since usually $\beta_L\ll\beta_G$:

$$\beta T\frac{DP}{Dt}\approx\frac{\beta_G}{\rho_G}\left(\dot{m}_{GU}+\dot{m}_{Gz}\right)\frac{T}{A}\frac{dP}{dz} \tag{23}$$

that is, the expansivity term in the energy equation is due to the expansivity of the gas phase inside the unit cell and the one crossing the borders of the control volume.

Viscous dissipation

Term (IV) of eq. (8) represents the viscous dissipation of energy and can be written as (Simões et al., 2014):

$$\mu\Phi\approx\mu\left(\frac{\partial u}{\partial y}\right)^2\approx\sum_{\phi\psi}\tau_{\phi\psi}\frac{S_{\phi\psi}}{A}\frac{L_\psi}{L_U}u_{\phi\psi} \tag{24}$$

The contributions of the viscous dissipation in each unit cell structure shall be averaged in terms of the region lengths, term L_ψ/L_U. Separating the contributions of the slug, film, elongated bubble and gas-liquid interface:

$$\mu\Phi\approx\frac{1}{AL_U}\left[\tau_{LS}S_{LS}L_S U_{LS}+\tau_{LB}S_{LB}L_B U_{LB}+\tau_{GB}S_{GB}L_B U_{GB}+\tau_i S_i L_B\left(U_{GB}-U_{LB}\right)\right] \tag{25}$$

Temperature distribution and mixture heat transfer coefficient

Substituting eqs. (17), (18) and (23) in (8) – the energy balance of the entire unit cell – and then multiplying by the unit cell volume $\forall = AL_U$:

$$\rho_m c_{P,m} AL_U U_T \frac{dT}{dz} + \left(\dot{m}_{Lz} c_{P,L} + \dot{m}_{Gz} c_{P,G}\right)\kappa\left(T_W - T\right) = \left(h_{GB} S_{GB} L_B + h_{LB} S_{LB} L_B + h_{LS} S_{LS} L_S\right)\left(T_W - T\right) + \frac{\beta_G}{\rho_G}\left(\dot{m}_{GU} + \dot{m}_{Gz}\right) TL_U \frac{dP}{dz} + \tau_{LS} S_{LS} L_S U_{LS} + \tau_{LB} S_{LB} L_B U_{LB} + \tau_{GB} S_{GB} L_B U_{GB} + \tau_i S_i L_B \left(U_{GB} - U_{LB}\right) \tag{26}$$

Equation (26) can be rewritten as:

$$m\frac{dT}{dz} + nT = p \tag{27}$$

$$m = \rho_m c_{P,m} AL_U U_T \tag{28}$$

$$n = q - \frac{\beta_G}{\rho_G}\left(\dot{m}_{GU} + \dot{m}_{Gz}\right) L_U \frac{dP}{dz} \tag{29}$$

$$p = qT_W + \tau_{LS} S_{LS} L_S U_{LS} + \tau_{LB} S_{LB} L_B U_{LB} + \tau_{GB} S_{GB} L_B U_{GB} + \tau_i S_i L_B \left(U_{GB} - U_{LB}\right) \tag{30}$$

$$q = \left(h_{GB} S_{GB} L_B + h_{LB} S_{LB} L_B + h_{LS} S_{LS} L_S\right) - \left(\dot{m}_{Lz} c_{P,L} + \dot{m}_{Gz} c_{P,G}\right)\kappa \tag{31}$$

Equation (27) is a first-order non-homogeneous ODE for the mixture temperature in terms of the axial pipe coordinate, whose solution for two consecutive nodes is:

$$T_{(n+1)} = \frac{p}{n} + \left(T_{(n)} - \frac{p}{n}\right)\exp\left(-\frac{n}{m}\Delta z\right) \tag{32}$$

Comparing the term inside the exponential with a homogeneous mixture solution for the energy balance, terms *n* and *m* can be related to the mixture heat transfer coefficient as (Bassani et al., 2016):

$$\frac{h_m S}{\dot{m}_m c_{P,m}} \approx \frac{n}{m} = \frac{\left(h_{GB} S_{GB} L_B + h_{LB} S_{LB} L_B + h_{LS} S_{LS} L_S\right) - \left(\dot{m}_{Lz} c_{P,L} + \dot{m}_{Gz} c_{P,G}\right)\kappa - \frac{\beta_G}{\rho_G}\left(\dot{m}_{GU} + \dot{m}_{Gz}\right) L_U \frac{dP}{dz}}{\rho_m c_{P,m} AL_U U_T} \tag{33}$$

Knowing that the mixture mass flow rate is $\dot{m}_m = \rho_m JA$ and isolating the mixture heat transfer coefficient:

$$h_m = \left\{ \underbrace{h_{GB}\frac{S_{GB}}{S}\frac{L_B}{L_U} + h_{LB}\frac{S_{LB}}{S}\frac{L_B}{L_U} + h_{LS}\frac{S_{LS}}{S}\frac{L_S}{L_U}}_{\text{convective terms (França et al., 2008)}} - \underbrace{\frac{\dot{m}_{Lz} c_{P,L} + \dot{m}_{Gz} c_{P,G}}{SL_U}\kappa}_{\text{scooping term}} - \underbrace{\frac{\beta_G}{\rho_G}\left(\dot{m}_{GU} + \dot{m}_{Gz}\right)\frac{1}{S}\frac{dP}{dz}}_{\text{expansivity term}} \right\} \frac{J}{U_T} \tag{34}$$

that is, the mixture heat transfer coefficient is a combination of: (i) the convective terms between the structures and the wall (França et al., 2008); (ii) the thermal scooping phenomenon – similar to Bassani et al. (2016), but accounting for the gas contribution; and (iii) the gas expansivity term (present work). It should be noticed, at this point, that the pressure gradient along the pipeline is a negative value, that is, $dP/dz < 0$. Also, for horizontal and inclined ascendant flows, usually $U_T > U_{\phi\psi}$, resulting in $\dot{m}_{\phi z} < 0$. Substituting these negative signs in eq. (34) and using the absolute values for those parameters:

$$h_m = \left\{ h_{GB}\frac{S_{GB}}{S}\frac{L_B}{L_U} + h_{LB}\frac{S_{LB}}{S}\frac{L_B}{L_U} + h_{LS}\frac{S_{LS}}{S}\frac{L_S}{L_U} + \frac{\left|\dot{m}_{Lz}\right| c_{P,L} + \left|\dot{m}_{Gz}\right| c_{P,G}}{SL_U}\kappa + \frac{\beta_G}{\rho_G}\left(\dot{m}_{GU} - \left|\dot{m}_{Gz}\right|\right)\frac{1}{S}\left|\frac{dP}{dz}\right| \right\} \frac{J}{U_T} \tag{35}$$

Therefore, two conclusions can be drawn from eq. (35): (i) the thermal scooping phenomenon is directly proportional to the heat transfer coefficient and (ii) the expansivity term is directly proportional to the heat transfer coefficient, since usually $\left|\dot{m}_{GU}\right| > \left|\dot{m}_{Gz}\right|$.

Constant external temperature boundary condition

So far, no mention has been made to the external temperature T_{ext}, only to the inner wall temperature T_W. Both temperatures are related through a radial thermal circuit as (Bassani et al., 2016):

$$T_W = T + \frac{D}{D_{ext}}\left[\frac{h_{LB}^{ov.}}{h_{LB}}\frac{L_B}{L_U} + \frac{h_{LS}^{ov.}}{h_{LS}}\frac{L_S}{L_U}\right]\left(T_{ext} - T\right) \tag{36}$$

where the overall heat transfer coefficient of the structures is expressed in terms of the internal mixture convection, the wall conduction and the external medium convection:

$$h_{\phi\psi}^{ov.} = \left[\underbrace{\frac{1}{h_{\phi\psi}}}_{\substack{\text{internal convection}\\ \text{of the mixture}}} + \underbrace{\frac{D\ln\left(D_{ext}/D\right)}{2k_W}}_{\text{pipe wall conduction}} + \underbrace{\frac{D}{D_{ext}h_{ext}}}_{\substack{\text{external medium}\\ \text{convection}}}\right]^{-1} \tag{37}$$

where k_W is the wall thermal conductivity, D_{ext} is the pipe external diameter and h_{ext} is the external medium heat transfer coefficient.

4. RESULTS AND DISCUSSIONS

The aim of this section is to answer the following questions:

(A) Is the gas energy really negligible for low pressure scenarios – near ambient conditions – as proposed originally by Bassani et al. (2016)?

(B) Does the present work model converges to the original model of Bassani et al. (2016) for low pressure scenarios? That is, are they equivalent to those cases and is really the present work an extension of the original one?

(C) What are the differences in the slug flow hydrodynamics and heat transfer brought by the consideration of the gas contribution to momentum and energy balances for long distance pipelines – that is, higher pressure conditions, near offshore operations (up to 300 bar)?

For this purpose, both models – the original (Bassani et al., 2016) and the one herein presented – will be compared in two distinct scenarios: (i) a short pipeline (50 m) with a low pressure at the inlet (2 bar) and (ii) a long pipeline (1.5 km) with a relatively high pressure at the inlet (300 bar). The input data for the model evaluation in both scenarios is presented in Table 1. The low pressure scenario has a gas/liquid (methane/water) density ratio of ≈ 1.3% at the pipe inlet, whereas the high pressure scenario has ≈ 21%. A small diameter pipe, with small wall width and high conductivity was chosen to intensify heat transfer, thus making differences on results more perceptible.

Table 1 – Input data for model evaluation.

Parameter	***Low pressure***	***High pressure***
Pipeline length	50 m	1.5 km
Internal diameter / Wall width	26 mm / 1 mm	
Wall thermal conductivity	400 W/(m.K) (copper)	
Fluids	Methane / Water	
Liquid and gas superficial velocities at the inlet	1 m/s and 1 m/s	
Pressure at the inlet	2 bar	300 bar
Gas/liquid density ratio	~1.3%	~21.0%
Temperature at the inlet / External medium temperature	25ºC / 4ºC (298 K / 277 K)	
External medium heat transfer coefficient	100 W/(m²K)	

Figure 2 presents a comparison between the present and the original models for the low pressure case. Results are shown for (a) temperature, (b) mixture heat transfer coefficient, (c) pressure and (d) gas superficial velocity. It can be observed that both models behave similarly when pressure is low. That is, the gas contribution can be neglected since $\rho_G \ll \rho_L$ in this case. Therefore, the answer to question (A) is: yes, gas energy can be neglected for low pressure scenarios (keeping in mind that the gas herein evaluated – methane – is quite light at this pressure, with $\rho_G/\rho_L \approx 1\%$). The only parameter that shows a slight difference between both models is the mixture heat transfer coefficient. The heat exchange between the gas phase and the wall represents a slight increase in the mixture heat transfer coefficient, around 0.3%. However, this difference is not representative and can be neglected for engineering purposes.

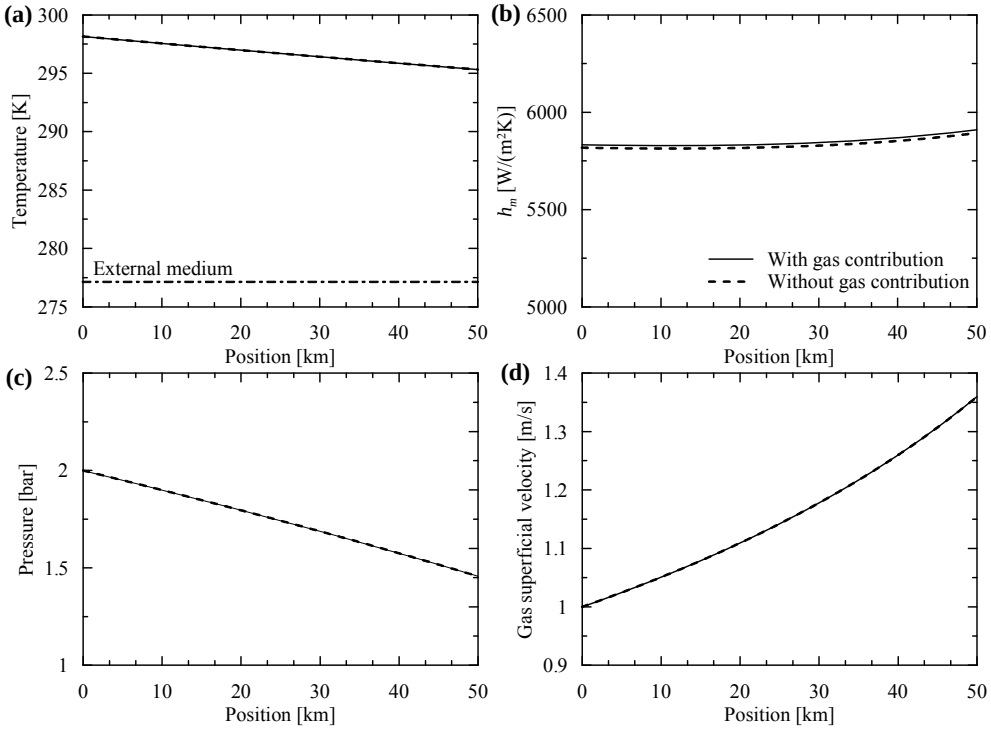

Figure 2 – Evaluation of gas contribution in: (a) mixture temperature, (b) mixture heat transfer coefficient, (c) mixture pressure and (d) gas superficial velocity. Distributions along the pipeline for the low pressure case (2 bar at the 50-m pipe inlet).

The answer to question (B) also comes from Fig. 2: yes, the present and the original models converge for low pressure scenarios, meaning that comparisons with experimental data made by Bassani et al. (2016) are valid for the present model. Comparisons with experimental data of Lima (2009) (air-water near ambient conditions) and literature correlations (Chisholm, 1967; García et al., 2007; Kim and Ghajar, 2006) showed model prediction accuracies of: ±35% for the temperature drop, ±25% for the mixture heat transfer coefficient, ±20% for the pressure gradient and ±10% for the mean liquid volumetric fraction. Experimental data for higher pressure conditions are not available in the literature, thus a proper validation of the presented model is not yet possible. The model can however be used to discuss, theoretically, the effects brought by the gas consideration into the slug flow behavior.

Figure 3 shows the same comparison made in Fig. 2, but for the high pressure case. The energy balance undergoes two competitive phenomena when the gas contribution is taken into consideration:

(i) The heat exchanged between the mixture and the wall increases, since the gas exchanges heat radially with the wall and axially between two consecutive unit cells (thermal scooping phenomenon). In Fig. 3b, it can be seen that the gas contribution increases the mixture heat transfer coefficient by approximately 22%.

(ii) Since the volumetric flow rate of the phases is kept constant for both cases (low and high pressure), then the high pressure case has a higher mixture mass flow rate (since ρ_G is higher). As a consequence, the mixture heat capacity – that is, the resistance of the mixture changing its temperature – is higher.

From the temperature distribution shown in Fig. 3a, it is clear that mechanism (ii) prevails over mechanism (i) for the evaluated case, and the temperature drop decreases when the gas is considered in the energy balance for the high pressure case.

Figure 3c shows that the terms due to friction between the gas and wall and at the gas/liquid interface are related to an increase in pressure drop for the high pressure case. Pressure drop is increased in approximately 15% when the gas is considered.

Figure 3d shows the gas superficial distribution along the pipeline. The trend of the gas superficial velocity is influenced by the competition between: (i) gas contraction due to the mixture cooling and (ii) gas expansion due to pressure drop. Since the mixture cooling is maximum at the pipe inlet – where $(T_W - T)$ is higher – the gas superficial velocity tends to decrease at this region, as the gas shrinkage effect due to the temperature drop surmounts the gas expansion effect due to the pressure drop. A minimum is reached when both phenomena cancel out themselves. Downstream this point, pressure drop prevails and the gas superficial velocity increases. Since temperature and pressure distribution change due to the consideration of the gas contribution on the energy and momentum balances, then the trend of the gas superficial velocity is also affected. Both phenomena – the temperature drop decrease and the pressure drop increase – tend to increase the gas superficial velocity. However, from Fig. 3d, it is noticed that the gas superficial

velocity is smaller when considering the gas contribution. This is actually due to the consideration of the real gas behavior through the use of the compressibility factor in eq. (6). The original model of Bassani et al. (2016) assumed an ideal behavior when recalculating the gas superficial velocity along the pipeline, which is not a valid assumption for the high pressure scenario.

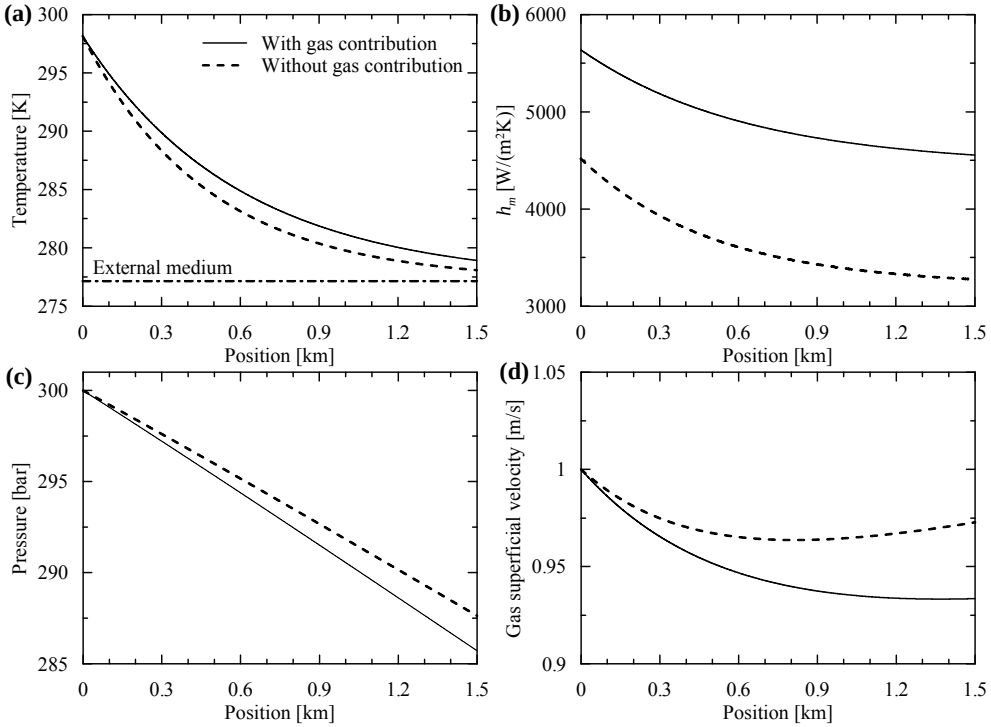

Figure 3 – Evaluation of gas contribution in: (a) mixture temperature, (b) mixture heat transfer coefficient, (c) mixture pressure and (d) gas superficial velocity. Distributions along the pipeline for the high pressure case (300 bar at the 1.5-km pipe inlet).

Finally, from Figure 3, the answer for question (C) can be obtained. In brief, the gas contribution to high pressure scenarios affects slug flow as follows: (i) temperature drop decreases due to an increase in the mixture heat capacity (assuming a constant volumetric flow rate), (ii) mixture heat transfer coefficient increases due to heat exchange of the gaseous phase with the wall, (iii) pressure drop increases due to gas friction and (iv) gas superficial velocity decreases due to the real-gas behavior of the gaseous phase.

5. CONCLUSIONS

The present study extended a mechanistic model for liquid-gas slug flows with heat transfer to consider the gas contribution to the momentum and energy balances. The gas contribution – neglected in the original model for low pressure scenarios, near ambient conditions and when $\rho_G/\rho_L \ll 1$ – cannot be neglected for higher pressures and consequently higher ρ_G/ρ_L ratios. The present and the original models converge for low pressure scenarios; thus, the validation made through comparison with experimental data in the original work is valid for the present study on low pressure scenarios. However, experimental data for high pressure scenarios is not available for validating the presented model. Therefore, this study discusses, theoretically, what are the differences due to the consideration of the gas contribution to the slug flow hydrodynamics and heat transfer in higher pressure scenarios. The consideration of the gas contribution implies in: (i) a temperature drop decrease due to an increase in the mixture heat capacity (assuming a constant volumetric flow rate), (ii) a mixture heat transfer coefficient increase due to gas heat transfer, (iii) a pressure drop increase due to gas friction and (iv) a gas superficial velocity decrease due to the real-gas behavior of the gaseous phase in higher pressure scenarios.

6. ACKNOWLEDGEMENTS

The authors acknowledge the financial support of ANP and FINEP through the Human Resources Program for Oil and Gas Segment PRHANP (PRH 10-UTFPR), TE/CENPES/PETROBRAS (0050.0068718.11.9) and National Council for Scientific and Technological Development (CNPq).

7. REFERENCES

Andreussi, P., Bendiksen, K.H., Nydal, O.J., 1993. Void distribution in slug flow. Int. J. Multiph. Flow 19, 817–828. doi:10.1016/0301-9322(93)90045-V

Bassani, C.L., Pereira, F.H.G., Barbuto, F.A.A., Morales, R.E.M., 2016. Modeling the scooping phenomenon for the heat transfer in liquid-gas horizontal slug flows. Appl. Therm. Eng. 98, 862–871. doi:10.1016/j.applthermaleng.2015.12.104

Chisholm, D., 1967. A theoretical basis for the Lockhart-Martinelli correlation for two-phase flow. Int. J. Heat Mass Transf. 10, 1767–1778. doi:10.1016/0017-9310(67)90047-6

Cook, M., Behnia, M., 2000. Pressure drop calculation and modelling of inclined intermittent gas-liquid flow. Chem. Eng. Sci. 55, 4699–4708. doi:10.1016/S0009-2509(00)00065-8

Danielson, T., 2011. A simple model for hydrodynamic slug flow, in: Offshore Technology Conference. Offshore Technology Conference, Houston/TX, USA. doi:10.4043/21255-MS

França, F.A., Bannwart, A.C., Camargo, R.M.T., Gonçalves, M.A.L., 2008. Mechanistic Modeling of the Convective Heat Transfer Coefficient in Gas-Liquid Intermittent Flows. Heat Transf. Eng. 29, 984–998. doi:10.1080/01457630802241091

García, F., García, J.M., García, R., Joseph, D.D., 2007. Friction factor improved correlations for laminar and turbulent gas-liquid flow in horizontal pipelines. Int. J. Multiph. Flow 33, 1320–1336. doi:10.1016/j.ijmultiphaseflow.2007.06.003

Harmathy, T.Z., 1960. Velocity of large drops and bubbles in media of infinite or restricted extent. AIChE J. 6, 281–288. doi:10.1002/aic.690060222

Issa, R.I., Kempf, M.H.W., 2003. Simulation of slug flow in horizontal and nearly horizontal pipes with the two-fluid model. Int. J. Multiph. Flow 29, 69–95. doi:10.1016/s0301-9322(02)00127-1

Kim, J.Y., Ghajar, A.J., 2006. A general heat transfer correlation for non-boiling gas-liquid flow with different flow patterns in horizontal pipes. Int. J. Multiph. Flow 32, 447–465. doi:10.1016/j.ijmultiphaseflow.2006.01.002

Kjeldby, T.K., Henkes, R. a W.M., Nydal, O.J., 2013. Lagrangian slug flow modeling and sensitivity on hydrodynamic slug initiation methods in a severe slugging case. Int. J. Multiph. Flow 53, 29–39. doi:10.1016/j.ijmultiphaseflow.2013.01.002

Lima, I.N.R.C., 2009. Estudo Experimental da Transferência de Calor no Escoamento Bifásico Intermitente Horizontal. Universidade Estadual de Campinas, São Paulo, Brazil.

Medina, C.D.P., Bassani, C.L., Cozin, C., Barbuto, F.A.A., Junqueira, S.L.M., Morales, R.E.M., 2015. Numerical simulation of the heat transfer in fully developed horizontal two-phase slug flows using a slug tracking method. Int. J. Therm. Sci. 88, 258–266. doi:10.1016/j.ijthermalsci.2014.05.007

Medina, C.D.P., Cozin, C., Morales, R.E.M., Junqueira, S.L.M., 2010. Hydrodynamics and heat transfer simulation for two-phase intermittent flow in horizontal pipes, in: 13th Braz. Congr. of Therm. Sci. and Eng. Uberlândia, Brazil.

Nydal, O.J., Banerjee, S., 1996. Dynamic slug tracking simulations for gas-liquid flow in pipelines. Chem. Eng. Commun. 141, 13–39. doi:10.1080/00986449608936408

Petalas, N., Aziz, K., 1998. A mechanistic model for multiphase flow in pipes, in: Annual Technical Meeting. Petroleum Society of Canada, Calgary, Canada. doi:10.2118/98-39

Schulkes, R., 2011. Slug frequencies revisited, in: 15th International Conference on Multiphase Production Technology. BHR Group, Cannes, France, pp. 311–325.

Shoham, O., 2006. Mechanistic modeling of gas-liquid two-phase flow in pipes, 1st ed. Society of Petroleum Engineers, Richardson, USA.

Simões, E.F., Carneiro, J.N.E., Nieckele, A.O., 2014. Numerical prediction of non-boiling heat transfer in horizontal stratified and slug flow by the two-fluid model. Int. J. Heat Fluid Flow 47, 135–145. doi:10.1016/j.ijheatfluidflow.2014.03.005

Taitel, Y., Barnea, D., 1998. Effect of gas compressibility on a slug tracking model. Chem. Eng. Sci. 53, 2089–2097. doi:10.1016/S0009-2509(98)00007-4

Taitel, Y., Barnea, D., 1990. A consistent approach for calculating pressure drop in inclined slug flow. Chem. Eng. Sci. 45, 1199–1206. doi:10.1016/0009-2509(90)87113-7

Zerpa, L.E., Rao, I., Aman, Z.M., Danielson, T.J., Koh, C.A., Sloan, E.D., Sum, A.K., 2013. Multiphase flow modeling of gas hydrates with a simple hydrodynamic slug flow model. Chem. Eng. Sci. 99, 298–304. doi:10.1016/j.ces.2013.06.016

8. RESPONSIBILITY NOTICE

The authors are the only responsible for the printed material included in this paper.